Title: Genotype and host microbiome alter competitive interactions between *Microcystis aeruginosa* and *Chlorella sorokiniana*.

Authors: Kathryn C. Schmidt[a], Sara L. Jackrel[a1], Derek Smith[b], Gregory J. Dick[a, b], Vincent J. Denef[a]

Author Affiliation: [a]Department of Ecology and Evolutionary Biology, University of Michigan, Ann Arbor, MI 48109, USA, [b]Department of Earth and Environmental Sciences, University of Michigan, Ann Arbor, MI 48109, USA, [1]Present Address: Sara L. Jackrel, Ecology, Behavior & Evolution Section, University of California San Diego, La Jolla, CA 92093, USA.

Corresponding author: Vincent Denef, 4060 Biological Sciences Building, 1105 North University Ave, Ann Arbor, MI 48109-1085, 734-764-6481, vdenef@umich.edu

Abstract: Cyanobacterial harmful algal blooms (cyanoHABs) continue to increase in frequency and magnitude, threatening global freshwater ecosystems and services. In north-temperate lakes cyanobacteria appear in early summer, succeeding green algae as the dominant phytoplankton group, a pattern thought to be mediated by changes in temperature and bioavailable nutrients. To understand additional drivers of this successional pattern our study used reciprocal invasion experiments to examine the competitive interaction between *Microcystis aeruginosa*, a dominant contributor to cyanoHABs, and the green alga *Chlorella sorokiniana*. We considered two factors that may impact these interactions: (1) strain variation, with a specific emphasis on the presence or absence of the gene for the hepatotoxin microcystin, and (2) host-associated bacteria. We used toxic *M. aeruginosa* PCC 7806 (microcystin producing strain), a non-toxic mutant of PCC 7806, non-toxic *M. aeruginosa* PCC

9701 (non-microcystin producing strain), and *C. sorokiniana.* Each organism was available free of all bacteria (i.e., axenic) and with a re-introduced defined bacterial community to generate their xenic counterparts. Competitive interactions were assessed with reciprocal invasion experiments between paired xenic and paired axenic populations of *C. sorokiniana* and one of the two *Microcystis* strains, each assessed separately. Flow cytometry and random forest models were used to rapidly discriminate and quantify phytoplankton population densities with 99% accuracy. We found that *M. aeruginosa* PCC 7806, but not strain PCC 9701, could proliferate from low abundance in a steady-state population of *C. sorokiniana*. Further, the presence of bacteria allowed *M. aeruginosa* PCC 7806 to grow to a higher population density into an established *C. sorokiniana* population than when grown axenic. Conversely, when *M. aeruginosa* was dominant, *C. sorokiniana* was only able to proliferate from low density into the PCC 9701 strain, and only when axenic. The mutant of PCC 7806 lacking the ability to produce microcystin behaved similarly to the toxic wild-type, implying microcystin is not responsible for the difference in competitive abilities observed between the two wild-type strains. Quantification of microcystins (MCs) when PCC 7806 *M. aeruginosa* was introduced into the *C. sorokiniana* culture showed two-fold more MCs per cell when host-associated bacteria were absent compared to present in both species cultures. Our results show that the ability of *M. aeruginosa* to compete with *C. sorokiniana* is determined by genomic differences beyond genes involved in microcystin toxin generation and indicate an important role of host-associated bacteria in mediating phytoplankton interspecies interactions. These results expand our understanding of the key drivers of phytoplankton succession and the establishment and persistence of freshwater harmful cyanobacterial blooms.

Keywords: interspecific interactions, microbiome, harmful algal bloom, competition, microcystin

1. Introduction

Cyanobacterial harmful algal blooms (cyanoHABs) in freshwater systems are increasing globally in frequency and magnitude due to human-caused eutrophication, rising temperatures, and changing weather and phenological patterns, including regional ice coverage, duration of stratification, and hydrology (Huisman *et al.* 2004; Paerl and Huisman 2008 and 2009; Paerl *et al.* 2016; Lürling *et al.* 2018). CyanoHABs impact ecosystem function by depleting bioavailable nutrients, causing localized hypoxia after their demise (Zilius *et al.* 2015; Watson *et al.* 2016), and by altering the physicochemical environment through the release of secondary metabolites (Cirri and Pohnert, 2019). These impacts of cyanoHABs can generate cascading effects through trophic levels (Huisman *et al.* 2018). Freshwater cyanoHABs are often dominated by *Microcystis aeruginosa* (Harke *et al.* 2016), which can release an array of secondary metabolites, including the hepatotoxin microcystin, that can negatively affect water quality essential for animal and human health.

Cyanobacteria are globally distributed in freshwater environments and naturally co-occur with eukaryotic phytoplankton (Zhou *et al.* 2018). In north temperate lakes, cyanobacteria are a normal component of phytoplankton succession, typically following early summer dominance by green algae (Sommer *et al.* 1989). This pattern has historically been driven by changes in temperature and the bioavailability of nitrogen and phosphorus (Sommer *et al.* 1989; Domis *et al.* 2007). However, anthropogenic changes in climate and land-use have led to increased temperatures and nutrient loading that have altered the environment and conditions that favor the proliferation of cyanoHABs (Paerl and Otten, 2013a). Recent marker gene and genomic studies have revealed that cyanoHABs, particularly *Microcystis aeruginosa*, contain significant within-species genetic diversity between freshwater systems, and across space and time within a single long-term bloom. This includes variation in strain toxicity (Kardinaal *et al.* 2007a, 2007b; Berry *et al.* 2017; Pérez-Carrascal *et al.* 2019; Jankowiak *et al.* 2019), mechanisms to overcome nutrient limitation including carbon-concentrating mechanisms and phosphate transporters

(Sandrini *et al.* 2014; Sandrini *et al.* 2016a, 2016b; Visser *et al.* 2016; Jackrel *et al.* 2019), and variation in associated heterotrophic communities or microbiomes (Kim *et al.* 2019; Jackrel *et al.* 2019; Cook *et al.* 2020; Chun *et al.* 2020). Succession from toxic to non-toxic variants of *M. aeruginosa* has been shown in several thermally stratified lakes across the globe (Fastner *et al.* 2001; Kardinaal *et al.* 2007b; Welker *et al.* 2007; Dong *et al.* 2019; Chun *et al.* 2020). Various explanations have been offered to explain this succession pattern, including physicochemical factors that might benefit certain variants over others, such as light levels (Kardinaal *et al.* 2007a; Phelan and Downing, 2011), phosphonate and nitrate concentrations (Vézie *et al.* 2002; Harke and Golber, 2013; Wang *et al.* 2015), reactive oxygen species concentrations (Dziallas and Grossart, 2011b; Paerl and Otten, 2013a), and temperature (Davis *et al.* 2009; Dziallas and Grossart, 2011a, 2011b). Explanations for these successional patterns have also included biological factors, such as cyanophage lysis-mediated strain succession (Yoshida *et al.* 2008). However, in complex, natural environments a combination of these factors likely drives strain heterogeneity across time and space (Li and Li 2012; Chun *et al.* 2020).

Competitive interactions, determined by species and strain optimization to the above listed abiotic and biotic factors, are well understood to be essential in the limitation and control of nuisance phytoplankton (Tilman 1982; Tilman *et al.* 1997; Shea and Chesson, 2002). In this study we focus on competitive interactions between *Microcystis* variants and a robust green algal competitor, *Chlorella sorokiniana*. While many species of green algae co-occur with *Microcystis*, we use a model genus for green algae, *Chlorella* that has been used in studies examining competitive interactions with *M. aeruginosa* (Zhang *et al.* 2007; Wang *et al.* 2015; Ma *et al.* 2015; Song *et al.* 2017; Wang *et al.* 2017; Ji *et al.* 2017). In addition to resource competition, we also have to consider interference competition. Multiple studies have examined allelopathy in intraspecific interactions between toxic and non-toxic *Microcystis* variants (Kardinaal et al. 2007a), and interspecific interactions between *Microcystis* variants and other

100 phytoplankton, including green algae (Zang *et al.* 2007; Bittencourt-Oliveira *et al.* 2014; Ma *et al.*
101 2015; Song *et al.* 2017; Ji *et al.* 2017; Yang *et al.* 2018; Dong *et al.* 2019), and diatoms (Wang
102 *et al.* 2017). The biological function of microcystin in these interactions, and its function in
103 general, has been widely debated. Proposed theories for the role of microcystin include acting
104 as a primary and secondary metabolite (Schatz *et al.* 2007), an allelochemical (Waal *et al.* 2011;
105 Li and Li, 2012), protection against oxidative stress (Zilliges *et al.* 2011; Phelan and Downing,
106 2011; Paerl and Otten, 2013b; Hernando *et al.* 2016), and as a carbon allocation mechanism
107 (Jähnichen *et al.* 2007).

108 The outcomes of competitive interactions often depend on the environmental constraints
109 imposed, including the biotic environment. In this study, we focus on the role of host-associated
110 bacteria, or microbiomes, which are known to alter numerous physicochemical factors and
111 therefore may have similar impacts as physicochemical environmental conditions on the
112 interactions between their algal hosts. Heterotrophic bacteria are known to influence
113 phytoplankton host fitness, by altering the availability of micronutrients, remineralizing
114 macronutrients, and aiding in the assimilation of vitamins such as B12 (Cho *et al.* 2015;
115 reviewed in Seymour *et al.* 2017; Samo *et al.* 2018; Cirri and Pohnert, 2019). Metagenomic
116 studies of cyanobacteria microbiomes show divergence of associated taxa or functional genes
117 based on nutrient gradients, but to a lesser extent host genotype (Frischkorn *et al.* 2017; Jackrel
118 *et al.* 2019). Further, Cook *et al* (2020) provided evidence of a co-evolved interactome of
119 associated bacteria and *Microcystis* that is reinforced by complementary biochemical pathways.
120 Therefore, assessing the microbiome of *Microcystis* and other phytoplankton is critical in
121 understanding the physiological constraints on phytoplankton host fitness, and thus predicting
122 the outcome of interspecific interactions that lead to the proliferation of cyanoHABs.

123 Impacts of microbiomes on competitive interactions between their hosts have been
124 shown for green algae and plants (Siefert *et al.* 2018 and 2019; Jackrel *et al.* 2020), and here

we address whether they also impact interactions between the cyanoHAB forming species *Microcystis* and a model green alga species *C. sorokiniana*. To understand the interplay between genetic diversity within *Microcystis aeruginosa*, specifically the role of microcystin, and phytoplankton microbiomes in driving cyanobacterial bloom successional patterns, we performed competition experiments. During these experiments, we tested two main hypotheses: (i) *M. aeruginosa* strain variation, including the occurrence of the microcystin gene, alters the competitive outcome with *C. sorokiniana* due to the relative fitness advantage of microcystin production, and (ii) the presence of host-associated bacteria alters the competitive outcome between *C. sorokiniana* and the two *M. aeruginosa* populations by affecting host fitness. Throughout the study, we use the term microbiome to refer to an engineered bacterial community that associated with our phytoplankton hosts. During the competition experiments, we monitored phytoplankton population growth of the species using flow cytometry to rapidly discriminate and quantify population densities. We also quantified total microcystin content during competition experiments to determine the relative effects of toxin production and host-associated bacteria in mediating phytoplankton successional dynamics.

2. Materials & Methods

2.1. Phytoplankton cultures

We obtained three strains of *Microcystis aeruginosa* from the Pasteur Culture Collection of Cyanobacteria (Pasteur Institute, Paris, France). PCC 9701 is a non-microcystin producing strain, PCC 7806 is a microcystin-producing strain, and the *mcyB*- PCC 7806 mutant strain cannot synthesize microcystin due to a mutation of the microcystin synthetase gene (Dittmann *et al.* 1997). We obtained a strain of the green alga, *Chlorella sorokiniana* (UTEX 2805), from the University of Texas Culture Collection of Algae (UTEX; Austin, Texas, USA). We grew cultures of all strains in COMBO medium, a defined freshwater media for algae and zooplankton

(Kilham *et al.* 1998). All incubations were performed on shaker tables set to a continuous 80 RPM under a light intensity of 30 µmol photons m^{-2} s^{-1} set to a 16:8 h light:dark cycle and 20°C. This temperature represents an intermediate temperature optimum between favorable conditions for green algae and *Microcystis* that ensures that neither phytoplankton group are favored competitively (addressed in Nolan *et al*. 2019).

Our strain of *C. sorokiniana* had been stored long-term in a laboratory collection at the University of Michigan, where heterotrophic bacteria were observed within the algal phycosphere. All *M. aeruginosa* strains were purchased axenic and required no manipulation. *Chlorella sorokiniana* was rendered axenic following the protocol outlined in Jackrel *et al.* (2020). Briefly, this approach combines ultrasonication of phytoplankton to liberate host-associated bacteria and single-cell fluorescence-activated cell sorting of algae onto plated solid media. Plates were then sealed with breathe-easy films (Diversified Biotech), which allow for gas exchange and maintain sterility, and incubated until visible colonies were examined under a dissecting scope for heterotroph contamination (Pereira *et al.* 2011). Colonies of *C. sorokiniana* that appeared heterotroph-free were streaked on COMBO-agar. Single colonies of *C. sorokiniana* were then inoculated into sterile COMBO media to generate axenic stock cultures.

2.2. Confirming axenic state

Samples taken from each phytoplankton culture were stained with DAPI (4′-6-diamidino-2-phenylindole) and visualized for heterotroph contamination on an Axio Imager 2 Zeiss fluorescent microscope under 100X magnification with an oil immersion lens and DAPI filter (bandpass, 470/20 nm excitation; long pass, 515 nm emission). We confirmed the absence of culturable bacteria in axenic *M. aeruginosa* and *C. sorokiniana* cultures by streaking phytoplankton cultures on R2A agar plates. Plates were incubated in the dark at room temperature and visualized for heterotroph growth after 5 days. For *C. sorokiniana,* we confirmed the absence of heterotrophic bacteria, including those that could not grow on R2A

medium through colony PCR. We detail this protocol in Jackrel *et al.* (2020). We confirmed the absence of phytoplankton heterotrophs in stock and experimental cultures periodically using microscopy and DAPI staining.

2.3. Bacterial isolation and identification

We isolated host-associated bacteria from phytoplankton cultures using a culture-based approach to later generate host-specific defined bacterial communities. For *M. aeruginosa*, bacteria were isolated from the freshwater strain LE3 (Brittain *et al.* 2000) because the toxin-producing strain (PCC 7806) and non-toxin producing (PCC 9701) strains were purchased axenic, meaning the culture was unialgal and had no bacteria associated present in the culture. We chose to isolate bacteria from *M. aeruginosa* strain LE3 because this is an environmentally relevant strain isolated from Lake Erie, USA that has been previously used (Rinta-Kanto *et al.* 2009; Saxton *et al.* 2012). For *C. sorokiniana*, we isolated bacterial heterotrophs that were present in the xenic *C. sorokiniana* culture. Using aseptic technique, both phytoplankton cultures were streaked on R2A agar, which is a medium optimized for slow-growing bacteria in potable freshwater (Reasoner and Geldreich, 1985). Plates were incubated in the dark at room temperature for 2-5 days and streaked for colony isolation.

We extracted DNA from morphologically distinct colonies by dissolving a single colony in 10 µL nuclease-free water and incubating for 10 minutes at 100°C using the PCR Mastercycler (Nexus gradient). We amplified the 16S rRNA gene from the extracted DNA using the product supernatant as the PCR template with the universal primers 27F (5′-AGAGTTTGATCCTGGCTCAG-3′) and 1492R (5′-GGTTACCTTGTTACGACTT-3′). Each 25 µL PCR reaction contained 13 µL nuclease-free water, 10 µL NEBNext High-Fidelity 2X PCR Master Mix, 1 µL template, 0.5 µL 10 µM forward primer, and 0.5 µL 10 µM reverse primer. PCR conditions were as follows: 94°C for 3 min, 35 cycles of denaturation (94°C for 45 sec.), annealing (46°C for 60 sec.), and extension (72°C for 90 sec.), and a final extension at 72°C for

10 min. Amplified PCR products were analyzed by electrophoresis on a 1% agarose gel, purified using the QIAquick PCR Purification Kit (QIAGEN, Hilden, Germany), and sequenced with an Applied Biosystems 3730xl DNA Analyzer (University of Michigan DNA Sequencing Core, MI, USA). Sequences were compared to the NCBI Genbank database using default BLASTn parameters to identify the bacterial isolate with the highest nucleotide pairwise identity.

2.4. Engineering defined xenic cultures

Isolated bacteria were introduced to axenic phytoplankton to generate host-specific defined bacterial communities. Bacterial colonies were inoculated into sterile R2A broth and incubated at room temperature on shaker tables overnight, or until growth was visible. Bacterial densities were approximated based on optical density measurements at 600 nm (OD_{600}). Thirty microliters of each bacterial culture, with OD_{600} measurements ranging from 0.10-0.34, were spiked into 100 mL of axenic phytoplankton at a density of 10,000 cells mL^{-1}. Based on the number of bacteria we could culture, two bacterial heterotrophs isolated from the long-term culture of *C. sorokiniana* were added to axenic *C. sorokiniana* (isolates #1 and #2, Table 2), and three bacterial heterotrophs isolated from LE3 were added to axenic strains of toxic and non-toxic *M. aeruginosa* (isolates #3-5, Table 2). After bacteria were spiked into the axenic phytoplankton cultures, the cultures were incubated for two-weeks prior to starting experiments to allow bacteria to associate with their algal host. During the two-week incubation period, fresh COMBO media was added to phytoplankton cultures in order to maintain viable phytoplankton growth. Prior to introducing the second phytoplankton population, we confirmed the retention of the bacterial community via microscopy. As there was no evidence of density-dependent effects of the bacterial inoculum size on phytoplankton host fitness (Supp. Figure 1), we did not continue to monitor bacterial densities in the phytoplankton cultures.

2.5. Competition Experiments

After establishing axenic phytoplankton monocultures and their engineered xenic counterparts, we inoculated all cultures at 10,000 phytoplankton cells mL^{-1} in fresh COMBO media and incubated as described previously in section 2.1. We evaluated pairwise species interactions between *C. sorokiniana* and the toxic and non-toxic strain of *M. aeruginosa* in the presence versus absence of host-associated bacteria (i.e. a xenic culture interacting with xenic culture, and axenic culture interacting with axenic culture) using the mutual invasibility criterion (Chesson 2000). This approach has been frequently used to examine interspecific interactions that mediate species coexistence, and can be more broadly applied to understand competitive interactions that mediate natural successional turnover in phytoplankton communities (Siefert *et al.* 2019; Jackrel *et al.* 2020). This criterion uses an experimental approach in which a species pair, A and B, are grown in monoculture until reaching steady-state, which we define as the measurement at which chlorophyll-a fluorescence did not change significantly for two days. Subsequently, the second species is introduced at low density to determine whether it can exhibit growth in presence of the established species (i.e., whether it can invade the established culture). Phytoplankton monoculture growth was tracked by chlorophyll-a fluorescence using a plate reader (Biotek Multi Plate Reader) until steady-state growth was achieved (Supp. Figure 2**)**. From initial inoculation until steady-state, we assessed the effects of the phytoplankton microbiome on monoculture host fitness by estimating maximum growth rate and final carrying capacity. We tested pairwise species combinations of each of our phytoplankton pairs (PCC7806 and Chlorella, PCC9701 and Chlorella), but assessed only xenic phytoplankton against other xenic phytoplankton and only axenic phytoplankton against other axenic phytoplankton. Each treatment was examined in triplicate, with all replicates spatially randomized in a Percival incubator. Once steady state was reached for the resident species, the second phytoplankton population was introduced at a density of 10,000 phytoplankton cells mL^{-1}. To be able to track growth of each phytoplankton species when grown together, we differentiated and quantified cells of *C. sorokiniana* and *M. aeruginosa* using flow cytometry

(Attune NxT Acoustic Focusing Cytometer, Invitrogen, USA). Due to the results from this first experiment, we then conducted a second competition experiment between axenic *C. sorokiniana* and the *mycB*- mutant strain of *M. aeruginosa*, following the methods described above, to test explicitly the effect of the presence versus absence of the microcystin gene in the competitive outcome. To control for variation in competition outcome that may result due to time, phytoplankton monocultures and the pairwise interaction of PCC7806 and Chlorella were also assessed in triplicate and physically randomized in the Percival incubator.

2.6. Flow cytometry quantification

We used flow cytometry to distinguish between phytoplankton populations using multiple intrinsic cellular properties including morphology, internal complexity, and autofluorescence. Following flow cytometric procedures described extensively in Props *et al.* (2016), we excluded laser noise and characterized single-cells by cell size (forward scatter), granularity (side scatter), chlorophyll-b fluorescence (blue laser excitation 488 nm, emission 695/40 nm), and chlorophyll-a fluorescence (violet laser excitation 405 nm, emission 660/20 nm). All flow cytometric data was visualized in the R studio using the R package “Phenoflow” (Props *et al.* 2016). We tracked phytoplankton population densities over 19 days, and discriminated between populations using the Random Forest classifier for supervised demarcation (RandomF_FCS function in Phenoflow), described further in section 2.8.

2.7. Microcystin quantification

We also monitored cultures used in the first competition experiment for total microcystin content (i.e, combined intracellular and extracellular) using the Abraxis Microcystins/ Nodularins (ADDA) ELISA Kit (Warminster, PA, USA). This kit allows for a congener-independent detection of various microcystins with the LR-microcystin variant being the most toxic and common (Omidi *et al.* 2018). Cultures were sampled 15 days after the second phytoplankton population was

added, based on our findings that our phytoplankton populations reach steady-state growth at approximately two-weeks. For microcystin sampling, each treatment flask was gently mixed before pipetting 1 mL culture into a cryovial containing 5 µL of 25% glutaraldehyde. The cryovials were then snap frozen in liquid nitrogen and stored at -80°C until processed. To obtain total microcystin concentrations, samples were lysed using 3 freeze-thaw cycles and an Abraxis QuikLyse™ Kit. Samples were then immediately processed following the manufacturer's instructions for the ELISA assay.

2.8. Statistical analyses

For surveys on the effect of bacterial communities on host growth, we fit logistic growth models to estimates of phytoplankton population growth based on chlorophyll-a fluorescence measurements in monocultures with and without their associated microbiomes. We fit the model to each replicate to obtain multiple, individual calculations of phytoplankton maximum growth rate (µ) using the 'growthrates' package in R software (Petzoldt 2018). Estimates of carrying capacity for each monoculture replicate were estimated based on the average chlorophyll-a fluorescence during the last two days of growth (Figure 1). We ran a linear mixed effects model with day interacting with either axenic/xenic state or phytoplankton population identity as the fixed effects, and biological replicate as a random effect. P-values were calculated using the analysis of variance function in the "nlme" package (Pinheiro and Bates 2000; Supp. Table 1).

To rapidly and accurately estimate phytoplankton population densities based on flow cytometry characterization, we trained Random Forest models for each species interaction pair (i.e. *C. sorokiniana* and toxic *M. aeruginosa*). We used flow cytometric data from each monoculture population to train the Random Forest classifier. For each model we randomly downsampled to 10,000 cells per sample and used 75% of our training data to train the model and generated a new model for every three day increment to account for phenotypic shifts in the population over time. Samples were cross-validated 10 fold and repeated 3 times. The model

306 was tested on the remaining 25% of the training data. In the competition experiments, we
307 compared the ability of a population to grow when rare in an established population in the
308 axenic/xenic state using the linear mixed effect model and analysis of variance as described
309 above for monoculture growth. We also compared monoculture growth of the established
310 population versus growth in the presence of another population to account for potential false-
311 positive cell counts as a result of Random Forest model error.
312
313 **3. Results**
314 We isolated five bacteria from our xenic phytoplankton cultures, two derived from *C.*
315 *sorokiniana* and three from *M. aeruginosa* strain LE3 (Table 1). Based on the NCBI blast
316 database, the closest matches to the 16S rRNA gene sequence of our two *C. sorokiniana*-
317 associated isolates were *Variovorax paradoxus* (96 % identity) and *Pedobacter glacialis* (96.5
318 %), and to our three *M. aeruginosa*-associated isolates were *Aeromicrobium ponti* (97 %),
319 *Rhizobium sp.* (96.8 %), and *Blastomonas fulva* (97 %), respectively. We engineered defined
320 bacterial communities instead of using undefined bacterial communities to facilitate
321 interpretations of the potential role of the bacteria taxa and host genotype in determining
322 competitive interactions. We first examined the effect of host-associated bacteria on
323 phytoplankton fitness by comparing growth of axenic phytoplankton cultures and defined xenic
324 phytoplankton monocultures. From the logistic models, we found that our bacterial communities
325 had no significant effect on maximum growth rate for either *C. sorokiniana* or *M. aeruginosa*
326 strains in comparison to the axenic monoculture (Figure 1, p-values in Supp. Table 1). Final
327 carrying capacity for each monoculture was calculated on day 19 of growth and determined
328 based on chlorophyll-a fluorescence. The carrying capacity of *C. sorokiniana* decreased when in
329 the presence of its microbiome when compared to its axenic monoculture (p-value: 0.0141).
330 Inversely, the xenic population of toxic *M. aeruginosa* reached a higher carrying capacity than

the axenic population (p-value: 0.006). Host-associated bacteria had no effect on the final carrying capacity of the non-toxic *M. aeruginosa* strain (p-value: 0.29).

Random forest models were trained on each phytoplankton interaction pair (i.e. *C. sorokiniana* and PCC7806 *M. aeruginosa*) and compared multiple cytometric features, including forward scatter (proxy. for cell size), side scatter (granularity), chlorophyll-b fluorescence (blue laser excitation 488 nm, emission 695/40 nm), and chlorophyll-a fluorescence (violet laser excitation 405 nm, emission 660/20 nm) (Figure 2). When all cytometric features were taken together, our models consistently performed with 99% accuracy (Figure 2, panel C) across interaction pair and over the course of the experiment.

During the competition experiments we found that strain variation and host-associated bacteria altered the strength and in some cases the outcome of competition. When comparing the effect of strain variation among axenic phytoplankton cultures, we found that *C. sorokiniana* was only able to invade and proliferate in a steady-state population of the non-toxic *M. aeruginosa* strain PCC 9701 (Figure 3a). In the reverse interaction, when *C. sorokiniana* was the dominant population, only the toxic strain of *M. aeruginosa* (PCC 7806) was able to invade and proliferate, whereas the non-toxic *M. aeruginosa* strain (PCC 9701) was excluded (Figure 3a, *strain:day* interaction p-value: <0.0001, other significant interactions in Supp. Table 1). We found this trend in two out of the three biological replicate competitive interactions of toxic *M. aeruginosa* (PCC 7806) invading *C. sorokiniana*. In the replicate that did not follow this trend, the population was able to grow in an established culture of *C. sorokiniana*, however, did not reach as high of carrying capacity as the other two replicates. Additionally, one replicate, in the axenic state where *C. sorokiniana* is rare in an established culture of *M. aeruginosa* PCC 9701 was removed from our analysis due to bacterial contamination determined by microscopy.

Based on the differential competitive abilities of the toxic PCC 7806 and non-toxic PCC 9701 *M. aeruginosa* strains with *C. sorokiniana*, we ran a follow-up experiment to test whether this result was dependent on the occurrence of the microcystin toxin gene, or on other

phenotypic factors related to strain variation. To answer this question, we used a *mycB*- mutant of the toxic *M. aeruginosa* strain PCC 7806, which is deficient in microcystin production. We found that, similar to our observation for the wild-type strain, the *mycB*- mutant was able to invade and proliferate into a steady-state population of *C. sorokiniana* and in the reverse interaction, *C. sorokiniana* was unable to invade into a steady-state population of the mycB- mutant (p-value > 0.5, Figure 3b).

When examining the effect of host-microbiomes on phytoplankton competitive interactions, we found that the presence of host-associated bacteria altered the growth of the toxic *M. aeruginosa* strain when toxic *M. aeruginosa* was rare (nlme p-value: 0.006; lme4 Pr(>Chisq): 0.004), namely allowing toxic *M. aeruginosa* to reach a marginally higher final population density (p-value: 0.056) than when grown in the absence of host-associated bacteria (Figure 4). Similar to the axenic state, we found this trend in the xenic state in two out of the three biological replicate competitive interactions. However, in the axenic and xenic outlier replicates, the xenic culture remained the stronger competitor (Figure 4). These trends were also confirmed through monitoring phycocyanin fluorescence over the course of the experiment, in which an increase in phycocyanin fluorescence indicates an increase in *M. aeruginosa* population density (Supp. Figure 3). In the axenic/xenic outlier replicate there was no significant difference in phycocyanin fluorescence between *C. sorokiniana* growing in monoculture and growing in competition, further indicating it as an outlier. For the inverse interaction where *M. aeruginosa* was dominant, *C. sorokiniana* was unable to invade the toxic *M. aeruginosa* strain population in either the presence or absence of bacteria. However, *C. sorokiniana* was able to invade and persist in non-toxic *M. aeruginosa,* PCC 9701 in the axenic state (*state:day* interaction p-value: <0.0001), while xenic *M. aeruginosa* PCC 9701 resisted the invasion of xenic *C. sorokiniana*.

In the majority of our competition experiments, the introduction of a second population inhibited the population density of the established species. We found that when comparing the

steady-state population of phytoplankton in monoculture versus competition, inhibition of the resident population was particularly evident in the combinations where the invader successfully established. For example, the population density of the established species *C. sorokiniana* decreased over the course of the experiment in the xenic state, and maintained a lower population density in the axenic state when grown with the toxic *M. aeruginosa* strain in comparison to *C. sorokiniana* growing alone (i.e. monoculture) (Supp. Figure 4). Further, in the axenic state, the growth of PCC9701 was strongly inhibited by the invasion of *C. sorokiniana* relative to PCC9701 monoculture growth (Supp. Figure 4).

We quantified the total microcystin content (intracellular and extracellular) 15 days after the introduction of the invader. We chose this timeframe based on the observation that phytoplankton cultures reached steady-state growth after two weeks. Microcystin concentration per cell (µg/cell) was calculated by dividing microcystin content by toxic *M. aeruginosa* population density determined by flow cytometry. We found that when toxic *M. aeruginosa* invaded *C. sorokiniana* two-fold more microcystin per *M. aeruginosa* cell was present in the absence of host-associated bacteria (1.7×10^3 µg/cell) than in the presence of host-associated bacteria (8.5×10^4 µg/cell) (p-value: 0.02, Figure 5).

4. Discussion

The present study revealed that host-associated bacteria can alter the competitive interaction between *M. aeruginosa* and *C. sorokiniana*. The magnitude of these effects were dependent on strain variation within *M. aeruginosa*, as well as the direction of succession (i.e. cyanobacteria succeeding green algae, versus green algae succeeding cyanobacteria). While numerous studies have assessed the environmental and biotic factors contributing to *Microcystis* dominated cyanoHABs, our study provides experimental evidence that heterotrophic bacteria influence competitive interactions between phytoplankton, using an approach rooted in coexistence theory. These results support recent findings from *in situ* sampling and isolate

409 collections derived from the environment that heterotrophic bacteria play significant roles in
410 cyanobacterial metabolism and intraspecific niche divergence (Jackrel *et al.* 2019; Cook *et al.*
411 2020) that likely govern interspecific interactions among phytoplankton.

412 Stable coexistence of two species requires capability for mutual invasion, i.e., that either
413 species can grow from low density in the presence of an established population of the other
414 species (Chesson, 2000). Results from our competition experiments, independent of the strain
415 used, never showed mutual invasion capabilities, suggesting that *M. aeruginosa* strains and *C.*
416 *sorokiniana* are unable to stably coexist within a homogenous/mixed, nutrient replete
417 environment. This result supports findings by Ma *et al.* (2015) that axenic strains of toxic *M.*
418 *aeruginosa* FACHB-905 and non-toxic *M. aeruginosa* FACHB-469 are unable to stably coexist
419 with *Chlorella vulgaris* in mesocosm conditions in temperatures ranging 20 to 25°C. The mutual
420 invasibility experimental criterion has been widely used to study the theory of phytoplankton
421 coexistence, but it can be more broadly applied to assess interspecific interactions that underlie
422 environmental phenomena. Specifically, the ability of a species to proliferate in the presence of
423 an established population mirrors phytoplankton successional patterns in some environments,
424 such as in north-temperate lakes where green algae reach peak abundance in early spring
425 followed by cyanobacteria (Sommer *et al.* 1989). According to stochastic niche theory, the
426 invading species, such as *M. aeruginosa*, can become established only if the population can
427 survive stochastic mortality while growing on the resources unused by the established species,
428 such as *C. sorokiniana* (Tilman, 2004). In our competition experiments, we mimicked eutrophic
429 environmental conditions by growing *M. aeruginosa* and *C. sorokiniana* cultures in nutrient rich
430 COMBO media without media replenishment. In this setup, we can conclude that if a second
431 population can establish when rare, where among species intraspecific competition is limited,
432 this must be due either to (1) relative fitness differences between the two species, which give
433 way to competitive hierarchies (i.e. resource uptake efficiency), or (2) niche differences between
434 the two species that offset competitive differences in population growth. While we found no

435 evidence for bi-directional invasibility among our phytoplankton interactions, unidirectional
436 invisibility suggests relative fitness differences between our phytoplankton populations, with the
437 most likely explanation being differential ability to access light or nutrients, although we could
438 not explicitly quantify these factors based on our experimental design.

439 Host microbiomes are known to alter the physiology and response of their phytoplankton
440 hosts to their environment (Ramanan *et al.* 2016; Frischkorn *et al.* 2017; Cirri and Pohnert,
441 2019), and are therefore suspected to play key roles in mediating phytoplankton between
442 species interspecific interactions during harmful algal blooms (Seymour *et al.* 2017). These
443 interactions between phytoplankton and bacteria, although occurring on a scale of microns, can
444 exert ecosystem-scale effects on biogeochemical cycling, nutrient cycling, primary productivity,
445 and toxin production (Buchan *et al.* 2014; reviewed in Seymour *et al.* 2017; Frischkorn *et al.*
446 2017). Specifically, heterotrophic bacteria have been shown to both augment and buffer the
447 effects of harmful algal blooms by enhancing the growth of HAB forming species, increasing
448 toxin production, and terminating HABs through the algicidal lysing of toxic phytoplankton (Bates
449 *et al.* 1995; Kodama *et al.* 2006; Sison-Mangus *et al.* 2013; Zhang *et al.* 2019). Similar to these
450 previous observations, our results show that host response to their biotic environment can be
451 modified by microbiomes. Specifically, bacteria provide a fitness advantage in competitive
452 interactions between *M. aeruginosa* and *C. sorokiniana*, as well as impact the concentration of
453 total microcystin.

454 The functional role of the microbiome in altering the ability of *Microcystis* strains and *C.*
455 *sorokiniana* to grow from low abundance in each other's presence was not explicitly tested. In
456 general, heterotrophs may directly and indirectly benefit their host in competitive interspecific
457 interactions. Associated heterotrophs remineralize macronutrients (Buchan *et al.* 2014), provide
458 vitamins and micronutrients (Amin *et al.* 2012), and compete for limited inorganic nutrients with
459 their phytoplankton host (Ramanan *et. al.*, 2016; Cook *et al.* 2020). Additionally, heterotrophs
460 can degrade toxic metabolic byproducts (Amin *et al.* 2012), produce algicidal compounds

(Kodama *et al.* 2006; Buchan *et al.* 2014), provide defense against pathogens through the interference of microbial signaling pathways (Satola *et al.* 2013), and could potentially use resources that may limit the proliferation of a competing species. Two bacterial families of which isolates were included in our study, *Sphingobacteriaceae* and *Comamonadaceae*, are commonly associated with green-algal cultures and their genes have been found to be highly transcribed within algal microbiomes sampled from the environment (Krohn-Molt *et al.* 2017). *Variovorax paradoxus* (family *Comamonadaceae*) isolated from *C. sorokiniana* is a common plant mutualist, thought to provide plant host protection against pathogens (Satola *et al.* 2013). Based on culture-dependent analyses, *Rhizobium* species are highly abundant in *M. aeruginosa* microbiomes, and have been found to promote host growth of axenic toxic *M. aeruginosa* PCC 7806 through catalase activity and the provision of fixed nitrogen resources (Kim *et al.* 2019). Additionally, *Blastomonas fulva* (family *Sphingobacteriaceae*) has been previously isolated from a *Microcystis* culture (Lee *et al.* 2017). The marginal decrease of the carrying capacity for *C. sorokiniana* relative to the axenic population may help explain why *C. sorokiniana* could no longer establish itself in the presence of the non-toxic *M. aeruginosa* strain PCC 9701 once bacteria were present, in addition to why establishment of the toxic *M. aeruginosa* strain into a *C. sorokiniana* culture was facilitated by the presence of host microbiomes. Hence, some of the more indirect benefits or emergent properties that arise from bacteria-bacteria interactions between the microbiomes of two hosts may help explain our observations. Additionally, the effect of the microbiome on host fitness may not be host specific (Jackrel *et al*., *in press*). Host microbiomes could affect competitive interactions not only by altering their host, but also by becoming associated over time with and altering the fitness of the second phytoplankton population.

Strain level variation within *M. aeruginosa* is extensive, with large variation in gene content between strains beyond the occurrence of microcystin biosynthesis genes (Humbert *et al.* 2013; Meyer *et al.* 2017; Pérez-Carrascal *et al.* 2019; Jackrel *et al.* 2019). Our results

487 suggest the toxic *M. aeruginosa* strain PCC 7806 is a more robust competitor relative to the
488 non-toxic *M. aeruginosa* strain PCC 9701, however this competitive edge is independent of the
489 ability to produce microcystin. The two specific strains we used vary from each other in the
490 ability to produce a series of secondary metabolites beyond microcystin. Specifically, the toxic
491 *M. aeruginosa* strain PCC 7806 contains genes related to the biosynthesis of aeruginosin and
492 the cytotoxic cyclic hexapeptide microcyclamide that are absent or incomplete in the non-toxic
493 *M. aeruginosa* strain PCC 9701 (Pérez-Carrascal *et al.* 2019). Conversely, the PCC 9701 strain
494 contains the complete biosynthetic gene cluster for the protease inhibitor Anabaenopeptin that
495 is absent in the PCC 7806 strain (Pérez-Carrascal *et al.* 2019). Our results support other
496 research that the competitive advantage of toxic *Microcystis* strains is not necessarily due to the
497 production of microcystin or microcystin acting as an allelopathic chemical (Briand *et al.* 2012;
498 Chia *et al.* 2018; Dong *et al.* 2019).

499 The concentration of cyanotoxins produced during cyanoHABs, specifically the
500 hepatotoxin microcystin, has direct implications for human and environmental health. We found
501 that the presence of host-microbiomes greatly reduced the concentration of microcystin per cell
502 relative to axenic competitive interactions. This could be either due to reduced production or due
503 to more rapid decay of microcystin due to bacterial biodegradation. Based on the data available,
504 we can only reasonably speculate regarding the potential of the heterotrophs in our engineered
505 microbiomes contributing to microcystin decay. Degradation of extracellular microcystin by
506 heterotrophic bacteria has been well supported both in the environment and laboratory settings
507 (Dziallas and Grossart, 2011a, Kormas and Lymperopoulou, 2013; Zhu *et al.* 2016; Thees *et al.*
508 2019). Specifically, the bacterium *Variovorax paradoxus* that we isolated from *C. sorokiniana* is
509 a known degrader of biogenic and anthropogenic compounds (Satola *et al.* 2013). Further, a
510 bacterial community from Lake Erie containing *V. paradoxus* was found capable of degrading
511 microcystin (Thees *et al.* 2019). Additionally, the bacterium *Blastomonas fulva* that we isolated
512 from *M. aeruginosa* belongs to the family *Sphingomonas*, which includes strains that are

513 capable of degrading cyanobacterial toxins, including LR-microcystin, and organic compounds
514 (Dziallas and Grossart, 2011a).

515 Through a combined approach of direct competition experiments and flow cytometry for
516 rapid cell quantification, we were able to readily assess the competitive interactions between
517 two phytoplankton populations under conditions that reflect population dynamics during
518 cyanoHABs. Previously, quantifying the competitive interaction between phytoplankton groups
519 has often relied on various, interdependent proxies of phytoplankton fitness, including the
520 correlation between chlorophyll-a biovolume and cell density (Briand *et al.* 2012; Nolan and
521 Cardinale, 2019). These approximations often lack accuracy at low cellular densities, due to
522 overlapping fluorescent spectra and difficulty decoupling chlorophyll/phycocyanin levels and cell
523 densities. The use of flow cytometry combined with machine learning approaches to
524 deconvolute the mixed signal from two co-occurring populations allowed us to rapidly quantify
525 population densities at the high temporal resolution needed to quantitatively assess the impact
526 of genotypic variation and the microbiome on phytoplankton competitive interactions (Rubbens
527 *et al.* 2019). In contrast to time-consuming manual counting, or less reliable fluorescence-based
528 proxy measurements, the flow cytometry approach increases throughput and likely increases
529 accuracy and reproducibility, especially of quantifying low population densities. While we did not
530 apply it here, flow cytometric population tracking also allows for the rapid enumeration of the
531 associated heterotrophic community. This method of accessing interspecific phytoplankton
532 interactions also has other promising applications, e.g., tracking of population-level phenotypic
533 shifts over time that has been previously applied to bacterioplankton communities (Props *et al.*
534 2018). Assessing competition through co-culturing methods rather than independent
535 measurements of fitness differences is also important as recent studies have shown stronger
536 inhibition in green algae growth when directly co-cultured with cyanobacteria (Wang *et al.* 2017;
537 Song *et al.* 2017).

We found that host microbiomes influence the competitive interaction of two phytoplankton species, however, there are several limitations and future directions that need to be addressed to understand the role of phytoplankton microbiomes in the proliferation and succession of *Microcystis* dominated cyanoHABs. Our study examined only a few bacterial taxa that we isolated from long-term laboratory cultures of phytoplankton, which generally harbor less diverse bacterial communities (Krohn-Molt *et al.* 2017; Kim *et al.* 2019) than phytoplankton-associated communities in the environment (Frischkorn *et al.* 2017). Similarly, community richness differed between *M. aeruginosa* (3 taxa) and *Chlorella* (2 taxa) microbiomes. Evenness of the bacterial community may also have fluctuated over time, as bacterial population densities were not tracked over the course of the experiment, limiting our understanding of the relative influence of bacterial community dynamics on phytoplankton host fitness and competitive interactions. Additionally, using a culture-based approach for bacterial isolation may represent a limited range of interactions between phytoplankton and their associated heterotrophs. We chose to use defined bacterial microbiomes during our fitness and competition assays to be better able to interpret our observations. Future studies are needed to gain a mechanistic understanding of how the microbiome influences competitive outcomes between phytoplankton species, and how these relationships differ across the many diverse genotypes relevant to *Microcystis* dominated cyanoHABs, and what the influence of microbiome composition variation is on these interactions. Additionally, the lab-based approaches used in our study are not representative of the full complexities of natural systems, where competitive outcomes are often attributed to a combination of bottom-up and top-down controls. Outcomes of our experiments and the extent of microbiome effects on phytoplankton fitness are dependent on the nutrient and experimental conditions provided, and outcomes may vary given different environmental conditions known to impact phytoplankton fitness, including temperature, light, and growth media. Further analyses of environmental conditions are necessary to determine the generality of these outcomes in nature. Our study suggests that host microbiomes may alter bottom-up

controls, i.e. interspecific competition for limited resources, or interference competition through production of allelochemicals, such as those seen in Song *et al.* (2017) in which *M. aeruginosa* inhibited growth of *Chlorella vulgaris* via positive feedback inhibition of linoleic acid. Yet, it does not take into account a number of top-down controls known to variably affect population dynamics among and within phytoplankton species in nature, including grazing by zooplankton (e.g., *Daphnia* spp. (Lemaire *et al.* 2012; Ekvall *et al.* 2016) and eukaryotic protists (Liu *et al.* 2012)), bivalves (reviewed in Harke *et al.* 2016), as well as viral mediated lysis (Yoshida *et al.* 2008).

Overall, understanding all the mechanisms that control phytoplankton interspecific interactions is critical in understanding the proliferation of nuisance phytoplankton species, and thus how community composition and ecosystem services will change in a world rapidly changed by anthropogenic disturbances (Paerl and Huisman, 2008; Paerl and Otten, 2013a; Jankowiak *et al.* 2019). Our study shows that the ability of *M. aeruginosa* to compete with *C. sorokiniana* is determined by the presence of host-associated microbiomes, as well as intraspecific genetic differences with *M. aeruginosa* beyond those genes specifically involved in microcystin toxin generation. Furthermore, our study describes the application of a promising method for examining population interactions, capable of including multiple phytoplankton species. These results using controlled lab-based experiments further support environmental observations and laboratory-based studies regarding the role of microbiomes in regulating host growth (Buchan *et al.* 2014; Cook *et al.* 2020) and provide new insights to the role of host microbiomes in mediating interspecific competitive interactions, and thus the succession of phytoplankton species during cyanoHABs.

Acknowledgements: We thank Lang Delancey and McKenzie Powers for help with phytoplankton culture growth. We also thank Ruben Props for help with flow cytometry data

589 analysis, Eric Bastien for Random Forest visualization analysis, and Natalie Imirzian for
590 preliminary tests of rendering algae axenic.
591
592 This work was funded by the UM M-Cubed Scholars program (to KCS) and by funding from the
593 NOAA Omics program distributed through the UM Cooperative Institute for Great Lakes
594 Research (NA17OAR4320152 to VJD and GJD).
595
596
597 **References:**

598 Amin, S. A., Parker, M. S., & Armbrust, E. V. (2012). Interactions between Diatoms and
599 Bacteria. *Microbiology and Molecular Biology Reviews*, *76*(3), 667–684.
600 Bates, S. S., Douglas, D. J., Doucette, G. J. & Léger, C. Enhancement of domoic acid
601 production by reintroducing bacteria to axenic cultures of the diatom Pseudo-nitzschia
602 multiseries. Nat. Tox. 3, 428–435 (1995).
603 Berry, M. A., White, J. D., Davis, T. W., Jain, S., Johengen, T. H., Dick, G. J., … Denef, V. J.
604 (2017). Are oligotypes meaningful ecological and phylogenetic units? A case study of
605 Microcystis in Freshwater lakes. *Frontiers in Microbiology*, *8*(MAR), 1–7.
606 Bittencourt-Oliveira, M. do C., Chia, M. A., de Oliveira, H. S. B., Cordeiro Araújo, M. K., Molica,
607 R. J. R., & Dias, C. T. S. (2014). Allelopathic interactions between microcystin-producing
608 and non-microcystin-producing cyanobacteria and green microalgae: implications for
609 microcystins production. *Journal of Applied Phycology*, *27*(1), 275–284.
610 Briand, E., Bormans, M., Quiblier, C., Salençon, M.-J., & Humbert, J.-F. (2012). Evidence of the
611 cost of the production of microcystins by Microcystis aeruginosa under differing light and
612 nitrate environmental conditions. *PLoS ONE*, *7*(1), e29981.
613 Brittain, S. M., J. Wang, L. Babcock-Jackson, W. W. Carmichael,K.L.Rinehart, andD.A.Culver.

(2000). Isolation and characterization of microcystins, cyclic heptapeptide hepatotoxins from a Lake Erie strain of Microcystis aeruginosa. J. Great Lakes Res. 26:241–249.

Buchan, A., LeCleir, G. R., Gulvik, C. A., & González, J. M. (2014). Master recyclers: features and functions of bacteria associated with phytoplankton blooms. *Nature Reviews. Microbiology*, *12*(10), 686–698.

Chesson, P. (2000). Mechanisms of maintenance of species diversity. *Annual Review of Ecology and Systematics*, *31*(1), 343–366.

Chia, M. A., Jankowiak, J. G., Kramer, B. J., Goleski, J. A., Huang, I. S., Zimba, P. V., … Gobler, C. J. (2018). Succession and toxicity of Microcystis and Anabaena (Dolichospermum) blooms are controlled by nutrient-dependent allelopathic interactions. *Harmful Algae*, *74*, 67–77.

Cho, D.-H., Ramanan, R., Heo, J., Lee, J., Kim, B.-H., Oh, H.-M., and Kim, H.-S. (2015) Enhancing microalgal biomass productivity by engineering a microalgal–bacterial community. Bioresour Technol. 175: 578–585.

Chun, S. J., Cui, Y., Lee, J. J., Choi, I. C., Oh, H. M., & Ahn, C. Y. (2020). Network analysis reveals succession of Microcystis genotypes accompanying distinctive microbial modules with recurrent patterns. *Water Research*, *170*, 115326.

Cirri, E., & Pohnert, G. (2019). Algae–bacteria interactions that balance the planktonic microbiome. *New Phytologist*, *223*(1), 100–106.

Cook, K. V., Li, C., Cai, H., Krumholz, L. R., Hambright, K. D., Paerl, H. W., … Zhu, G. (2020). The global Microcystis interactome. *Limnology and Oceanography*, *65*(S1), S194–S207.

Dittmann, E., Neilan, B. A., Erhard, M., von Döhren, H., & Börner, T. (1997). Insertional mutagenesis of a peptide synthetase gene that is responsible for hepatotoxin production in the cyanobacterium Microcystis aeruginosa PCC 7806. *Molecular Microbiology*, *26*, 779–787.

Dong, J., Li, C., Chang, M., Dai, D., Liu, S., Quan, B., … Gao, Y. (2019). Effects of toxic

cyanobacterium Microcystis aeruginosa on the morphology of green alga Chlorella vulgaris . *Annales de Limnologie - International Journal of Limnology*, *55*, 7.

Dziallas, C., & Grossart, H. P. (2011a). Temperature and biotic factors influence bacterial communities associated with the cyanobacterium Microcystis sp. *Environmental Microbiology*, *13*(6), 1632–1641.

Dziallas, C., & Grossart, H. P. (2011b). Increasing oxygen radicals and water temperature select for toxic microcystis sp. *PLoS ONE*, *6*(9).

Fastner, J., M. Erhard, and H. von Do¨hren. (2001). Determination of oligopeptide diversity within a natural population of Microcystis spp. (cyanobacteria) by typing single colonies by matrix-assisted laser desorption ionization–time of flight mass spectrometry. *Appl. Environ. Microbiol,* 67,5069–5076.

Frischkorn, K. R., Rouco, M., Van Mooy, B. A. S., & Dyhrman, S. T. (2017). Epibionts dominate metabolic functional potential of Trichodesmium colonies from the oligotrophic ocean. *The ISME Journal*, *11*(9), 2090–2101.

Harke, M. J., & Gobler, C. J. (2013). Global transcriptional responses of the toxic cyanobacterium, Microcystis aeruginosa, to nitrogen stress, phosphorus stress, and growth on organic Matter. *PLoS ONE*, *8*(7).

Harke, M. J., Steffen, M. M., Gobler, C. J., Otten, T. G., Wilhelm, S. W., Wood, S. A., & Paerl, H. W. (2016). A review of the global ecology, genomics, and biogeography of the toxic cyanobacterium, Microcystis spp. *Harmful Algae*, *54*, 4–20.

Huisman, J., Sharples, J., Stroom, J. M., Visser, P. M., Kardinaal, W. E. A., Verspagen, J. M. H., & Sommeijer, B. (2004). Changes in turbulent mixing shift competition for light between phytoplankton species. *Ecology*, *85*(11), 2960–2970.

Huisman, J., Codd, G. A., Paerl, H. W., Ibelings, B. W., Verspagen, J. M. H., & Visser, P. M. (2018). Cyanobacterial blooms. *Nature Reviews Microbiology*, *16*(8), 471–483.

Jackrel, S. L., White, J. D., Evans, J. T., Buffin, K., Hayden, K., Sarnelle, O., & Denef, V. J.

(2019). Genome evolution and host-microbiome shifts correspond with intraspecific niche divergence within harmful algal bloom-forming Microcystis aeruginosa. *Molecular Ecology*, *28*(17), 3994–4011.

Jackrel, S. L., Schmidt, K. C., Cardinale, B. J., & Denef, V. J. (2020). Microbiomes reduce their host's sensitivity to interspecific interactions. *MBio*, *11*(1), 1–11.

Jackrel, S.J., Yang, J., Schmidt, K.C., & Denef, V.J. Host-specificity of microbiome assembly and its fitness effects in phytoplankton. ISME J. (in press).

Jankowiak, J., Hattenrath-Lehmann, T., Kramer, B. J., Ladds, M., & Gobler, C. J. (2019). Deciphering the effects of nitrogen, phosphorus, and temperature on cyanobacterial bloom intensification, diversity, and toxicity in western Lake Erie. *Limnology and Oceanography*, *64*(3), 1347–1370.

Ji, X., Verspagen, J. M. H., Stomp, M., & Huisman, J. (2017). Competition between cyanobacteria and green algae at low versus elevated CO2: who will win, and why? *Journal of Experimental Botany*, *68*(14), 3815–3828.

Kardinaal, W. E. A., Tonk, L., Janse, I., Hol, S., Slot, P., Huisman, J., & Visser, P. M. (2007a). Competition for light between toxic and nontoxic strains of the harmful cyanobacterium Microcystis. *Applied and Environmental Microbiology*, *73*(9), 2939–2946.

Kardinaal, W. E. A., Janse, I., Kamst-Van Agterveld, M., Meima, M., Snoek, J., Mur, L. R., … Visser, P. M. (2007b). Microcystis genotype succession in relation to microcystin concentrations in freshwater lakes. *Aquatic Microbial Ecology*, *48*(1), 1–12.

Kilham, S. S., D. A. Kreeger, S. G. Lynn, C. E. Goulden, and L. Herrera. (1998). COMBO: a defined freshwater culture medium for algae and zooplankton. Hydrobiologia 377:147–159.

Kim, M., Shin, B., Lee, J., Park, H. Y., & Park, W. (2019). Culture-independent and culture-dependent analyses of the bacterial community in the phycosphere of cyanobloom-forming Microcystis aeruginosa. *Scientific Reports*, *9*(1), 1–13.

692 Kodama, M., Doucette, G. J., and Green, D. H. (2006). “Relationships between bacteria and
693 harmful algae,” in Ecology of Harmful Algae, Ecological Studies, Vol. 189, eds E. Granéli
694 and J. T. Turner (Berlin: Springer-Verlag), 243–255.
695 Krohn-Molt, I., Alawi, M., Förstner, K. U., Wiegandt, A., Burkhardt, L., Indenbirken, D., … Streit,
696 W. R. (2017). Insights into microalga and bacteria interactions of selected phycosphere
697 biofilms using metagenomic, transcriptomic, and proteomic approaches. *Frontiers in*
698 *Microbiology*, *8*(October), 1–14.
699 Lee, H.-G., Ko, S.-R., Lee, J.-W., Lee, C. S., Ahn, C.-Y., Oh, H.-M., & Jin, L. (2017).
700 Blastomonas fulva sp. nov., aerobic photosynthetic bacteria isolated from a Microcystis
701 culture. *International Journal of Systematic and Evolutionary Microbiology*, *67*(8), 3071–
702 3076.
703 Lemaire, V., Brusciotti, S., van Gremberghe, I., Vyverman, W., Vanoverbeke, J., & De Meester,
704 L. (2012). Genotype×genotype interactions between the toxic cyanobacterium Microcystis
705 and its grazer, the waterflea Daphnia. *Evolutionary Applications*, *5*(2), 168–182.
706 Li, Y., & Li, D. (2012). Competition between toxic Microcystis aeruginosa and nontoxic
707 Microcystis wesenbergii with Anabaena PCC7120. *Journal of Applied Phycology*, *24*(1),
708 69–78.
709 Lürling, M., Mello, M. M., van Oosterhout, F., Domis, L. de S., & Marinho, M. M. (2018).
710 Response of natural cyanobacteria and algae assemblages to a nutrient pulse and
711 elevated temperature. *Frontiers in Microbiology*, *9*(AUG), 1–14.
712 Ma, Z., Fang, T., Thring, R. W., Li, Y., Yu, H., Zhou, Q., & Zhao, M. (2015). Toxic and non-toxic
713 strains of Microcystis aeruginosa induce temperature dependent allelopathy toward growth
714 and photosynthesis of Chlorella vulgaris. *Harmful Algae*, *48*, 21–29.
715 Meyer, K. A., Davis, T. W., Watson, S. B., Denef, V. J., Berry, M. A., & Dick, G. J. (2017).
716 Genome sequences of lower Great Lakes Microcystis sp. reveal strain-specific genes that
717 are present and expressed in western Lake Erie blooms. *PLoS ONE*, *12*(10), 1–21.

718 Nolan, M. P., & Cardinale, B. J. (2019). Species diversity of resident green algae slows the
719 establishment and proliferation of the cyanobacterium Microcystis aeruginosa. *Limnologica*,
720 *74*(November 2018), 23–27.
721 Omidi, A., Esterhuizen-Londt, M., & Pflugmacher, S. (2018). Still challenging: the ecological
722 function of the cyanobacterial toxin microcystin – What we know so far. *Toxin Reviews*,
723 *37*(2), 87–105.
724 Paerl, H. W., & Huisman, J. (2008). Climate: Blooms like it hot. *Science*, *320*(5872), 57–58.
725 Paerl, H. W., & Huisman, J. (2009). Climate change: A catalyst for global expansion of harmful
726 cyanobacterial blooms. *Environmental Microbiology Reports*, *1*(1), 27–37.
727 Paerl, H. W., & Otten, T. G. (2013a). Harmful cyanobacterial blooms: Causes, consequences,
728 and controls. *Microbial Ecology*, *65*(4), 995–1010.
729 Paerl, H. W., & Otten, T. G. (2013b). Blooms bite the hand that feeds them. *Science*, *342*(6157),
730 433–434.
731 Pérez-Carrascal, O. M., Terrat, Y., Giani, A., Fortin, N., Greer, C. W., Tromas, N., & Shapiro, B.
732 J. (2019). Coherence of Microcystis species revealed through population genomics. *ISME*
733 *Journal*, *13*(12), 2887–2900.
734 Thomas Petzoldt (2018). growthrates: Estimate growth rates from experimental data. R package
735 version 0.7.2. https://CRAN.R-project.org/package=growthrates
736 Pereira, H., Barreira, L., Mozes, A., Florindo, C., Polo, C., Duarte, C. V, … Varela, J. (2011).
737 Microplate-based high throughput screening procedure for the isolation of lipid-rich marine
738 microalgae. *Biotechnology for Biofuels*, *4*(1), 61.
739 Phelan, R. R., & Downing, T. G. (2011). A growth advantage for microcystin production by
740 microcystis PCC7806 under high light. *Journal of Phycology*, *47*(6), 1241–1246.
741 Pinheiro, J. C. and Bates, D. M. (2000), Mixed-effects models in S and S-PLUS, Springer, New
742 York.
743 Props, R., Monsieurs, P., Mysara, M., Clement, L., & Boon, N. (2016). Measuring the

biodiversity of microbial communities by flow cytometry. *Methods in Ecology and Evolution*, *7*(11), 1376–1385.

Props, R., Schmidt, M. L., Heyse, J., Vanderploeg, H. A., Boon, N., & Denef, V. J. (2018). Flow cytometric monitoring of bacterioplankton phenotypic diversity predicts high population-specific feeding rates by invasive dreissenid mussels. *Environmental Microbiology*, *20*(2), 521–534.

Ramanan, R., Kim, B.-H., Cho, D.-H., Oh, H.-M., & Kim, H.-S. (2016). Algae–bacteria interactions: Evolution, ecology and emerging applications. *Biotechnology Advances*, *34*(1), 14–29.

Reasoner, D. J., & Geldreich, E. E. (1985). A new medium for the enumeration and subculture of bacteria from potable water. *Applied and Environmental Microbiology*, *49*(1), 1–7.

Rinta-Kanto, J. M., Saxton, M. A., DeBruyn, J. M., Smith, J. L., Marvin, C. H., Krieger, K. A., … Wilhelm, S. W. (2009). The diversity and distribution of toxigenic Microcystis spp. in present day and archived pelagic and sediment samples from Lake Erie. *Harmful Algae*, *8*(3), 385–394.

Rubbens, P., Schmidt, M. L., Props, R., Biddanda, B. A., Boon, N., Waegeman, W., & Denef, V. J. (2019). Randomized lasso links microbial taxa with aquatic functional groups inferred from flow cytometry. *MSystems*, *4*(5), 1–17.

Sandrini, G., Matthijs, H. C. P., Verspagen, J. M. H., Muyzer, G., & Huisman, J. (2014). Genetic diversity of inorganic carbon uptake systems causes variation in CO2 response of the cyanobacterium Microcystis. *ISME Journal*, *8*(3), 589–600.

Sandrini, G., Tann, R. P., Schuurmans, J. M., van Beusekom, S. A. M., Matthijs, H. C. P., & Huisman, J. (2016a). Diel variation in gene expression of the CO2-concentrating mechanism during a harmful cyanobacterial bloom. *Frontiers in Microbiology*, *7*(APR), 1–16.

Sandrini, G., Ji, X., Verspagen, J. M. H., Tann, R. P., Slot, P. C., Luimstra, V. M., … Huisman, J.

770 (2016b). Rapid adaptation of harmful cyanobacteria to rising CO2. *Proceedings of the*
771 *National Academy of Sciences of the United States of America*, *113*(33), 9315–9320.
772 Samo, T. J., Kimbrel, J. A., Nilson, D. J., Pett-Ridge, J., Weber, P. K., & Mayali, X. (2018).
773 Attachment between heterotrophic bacteria and microalgae influences symbiotic
774 microscale interactions. *Environmental Microbiology*, *20*(12), 4385–4400.
775 Satola, B., Wübbeler, J. H., & Steinbüchel, A. (2013). Metabolic characteristics of the species
776 Variovorax paradoxus. *Applied Microbiology and Biotechnology*, *97*(2), 541–560.
777 Saxton, M. A., Arnold, R. J., Bourbonniere, R. A., McKay, R. M. L., & Wilhelm, S. W. (2012).
778 Plasticity of total and intracellular phosphorus quotas in Microcystis aeruginosa cultures
779 and Lake Erie algal assemblages. *Frontiers in Microbiology*, *3*(JAN), 1–9.
780 Schatz, D., Keren, Y., Vardi, A., Sukenik, A., Carmeli, S., Börner, T., … Kaplan, A. (2007).
781 Towards clarification of the biological role of microcystins, a family of cyanobacterial toxins.
782 *Environmental Microbiology*, *9*(4), 965–970.
783 Seymour, J. R., Amin, S. A., Raina, J.-B., & Stocker, R. (2017). Zooming in on the phycosphere:
784 the ecological interface for phytoplankton–bacteria relationships. *Nature Microbiology*, *2*,
785 17065.
786 Shea, K., & Chesson, P. (2002). Community ecology theory as a framework for biological
787 invasions. *Trends in Ecology and Evolution*, *17*(4), 170–176.
788 Siefert, A., Zillig, K. W., Friesen, M. L., & Strauss, S. Y. (2018). Soil microbial communities alter
789 conspecific and congeneric competition consistent with patterns of field coexistence in
790 three Trifolium congeners. *Journal of Ecology*, *106*(5), 1876–1891.
791 Siefert, A., Zillig, K. W., Friesen, M. L., & Strauss, S. Y. (2019). Mutualists stabilize the
792 coexistence of congeneric legumes. *American Naturalist*, *193*(2), 200–212.
793 Sison-Mangus, M. P., Jiang, S., Tran, K. N., & Kudela, R. M. (2013). Host-specific adaptation
794 governs the interaction of the marine diatom, Pseudo-nitzschia and their microbiota. *The*
795 *ISME Journal Advance Online Publication*, *doi*(10).

796 Song, H., Lavoie, M., Fan, X., Tan, H., Liu, G., Xu, P., … Qian, H. (2017). Allelopathic
797 interactions of linoleic acid and nitric oxide increase the competitive ability of Microcystis
798 aeruginosa. *The ISME Journal*, *11*(8), 1865–1876.
799 Thees, A., Atari, E., Birbeck, J., Westrick, J. A., & Huntley, J. F. (2019). Isolation and
800 characterization of Lake Erie bacteria that degrade the cyanobacterial microcystin toxin
801 MC-LR. *Journal of Great Lakes Research*, *45*(1), 138–149.
802 Van De Waal, D. B., Verspagen, J. M. H., Finke, J. F., Vournazou, V., Immers, A. K., Kardinaal,
803 W. E. A., … Huisman, J. (2011). Reversal in competitive dominance of a toxic versus non-
804 toxic cyanobacterium in response to rising CO 2. *ISME Journal*, *5*(9), 1438–1450.
805 Vézie, C., Rapala, J., Vaitomaa, J., Seitsonen, J., & Sivonen, K. (2002). Effect of nitrogen and
806 phosphorus on growth of toxic and nontoxic Microcystis strains and on intracellular
807 microcystin concentrations. *Microbial Ecology*, *43*(4), 443–454.
808 Visser, P. M., Verspagen, J., Sandrini, G., Stal, L. J., Matthijs, H., Davis, T. W., Paerl, H. W., &
809 Huisman, J. (2016). How rising CO2 and global warming may stimulate harmful
810 cyanobacterial blooms. *Harmful algae*, *54*, 145–159.
811 Wang, L., Zi, J., Xu, R., Hilt, S., Hou, X., & Chang, X. (2017). Allelopathic effects of Microcystis
812 aeruginosa on green algae and a diatom: Evidence from exudates addition and co-
813 culturing. *Harmful Algae*, *61*, 56–62.
814 Watson, S. B., Miller, C., Arhonditsis, G., Boyer, G. L., Carmichael, W., Charlton, M. N., …
815 Wilhelm, S. W. (2016). The re-eutrophication of Lake Erie: Harmful algal blooms and
816 hypoxia. *Harmful Algae*, *56*, 44–66.
817 Yang, J., Tang, H., Zhang, X., Zhu, X., Huang, Y., & Yang, Z. (2018). High temperature and pH
818 favor Microcystis aeruginosa to outcompete Scenedesmus obliquus. *Environmental*
819 *Science and Pollution Research*, *25*(5), 4794–4802.
820 Yoshida, M., Yoshida, T., Kashima, A., Takashima, Y., Hosoda, N., Nagasaki, K., & Hiroishi, S.
821 (2008). Ecological dynamics of the toxic bloom-forming cyanobacterium Microcystis

822 aeruginosa and its cyanophages in freshwater. *Applied and Environmental Microbiology*,
823 *74*(10), 3269–3273.
824 Zhang, M., Kong, F., Xing, P., & Tan, X. (2007). Effects of interspecific interactions between
825 Microcystis aeruginosa and Chlorella pyrenoidosa on their growth and physiology.
826 *International Review of Hydrobiology*, *92*(3), 281–290.
827 Zhang, M., Lu, T., Paerl, H. W., Chen, Y., Zhang, Z., Zhou, Z., & Qian, H. (2019). Feedback
828 regulation between aquatic microorganisms and the bloom-forming cyanobacterium
829 Microcystis aeruginosa. *Applied and Environmental Microbiology*, *85*(21).
830 Zhou, J., Richlen, M. L., Sehein, T. R., Kulis, D. M., Anderson, D. M., & Cai, Z. (2018). Microbial
831 community structure and associations during a marine dinoflagellate bloom. *Frontiers in*
832 *Microbiology*, *9*(JUN), 1–21.
833 Zhu, L., Zuo, J., Song, L., & Gan, N. (2016). Microcystin-degrading bacteria affect mcyD
834 expression and microcystin synthesis in Microcystis spp. *Journal of Environmental*
835 *Sciences (China)*, *41*(Mc), 195–201.
836 Zilius, M., De Wit, R., & Bartoli, M. (2015). Response of sedimentary processes to
837 cyanobacteria loading. *Journal of Limnology*, *75*(2), 236–247.
838 Zilliges, Y., Kehr, J.-C., Meissner, S., Ishida, K., Mikkat, S., Hagemann, M., … Dittmann, E.
839 (2011). The cyanobacterial hepatotoxin microcystin binds to proteins and increases the
840 fitness of Microcystis under oxidative stress conditions. *PLoS ONE*, *6*(3), e17615.
841
842
843
844
845
846
847

848 **Figure Legends:**

849 **Figure 1**| The presence of host associated-heterotrophs had a mixed effect on phytoplankton
850 fitness as determined by maximum growth rate (μ_{max}) and carrying capacity (K) of the
851 monocultures. (**A**) The microbiome had no effect on the μ_{max} of their phytoplankton host in
852 monoculture. The μ_{max} of each of the three replicates were calculated from a parametric growth
853 model fit to chlorophyll-a raw fluorescence unit (RFU) measures using the "growthrates"
854 package in R. (**B**) The presence of the host-microbiome decreased K for *C. sorokiniana*
855 (Chlorella), increased K for toxic *M. aeruginosa* (PCC7806), and had no effect on the non-toxic
856 *M. aeruginosa* (PCC9701) strain. We calculated K by taking the average chlorophyll-a RFU for
857 each of the three replicates on day 18 and 19, when cultures were at steady-state growth. For
858 both **A** and **B**, axenic monocultures (black boxes) are compared to a xenic monoculture (light
859 grey boxes) containing a defined bacterial community. Asterisks indicate for which
860 phytoplankton cultures' axenic/xenic state significantly affected growth, determined by
861 performing an analysis of variance on a linear mixed model on the data. A single and double
862 black asterisk indicates P value of $\leq$0.05 and $\leq$0.01 respectively.
863
864 **Figure 2**| Phytoplankton populations were rapidly differentiated in competition experiments
865 using flow cytometry and a machine learning algorithm based on monoculture data. (**A**)
866 Absence of bacterial heterotrophs confirmed with microscopy of phytoplankton cultures.
867 Micrographs were taken at 1,000 X oil immersion magnification stained with DAPI ((4′-6-
868 diamidino-2-phenylindole) nucleic-acid stain and visualized under the DAPI filter (Axio Imager 2
869 Zeiss fluorescent microscope, bandpass, 470/20 nm excitation; long pass, 515 nm emission).
870 As these phytoplankton cultures are morphologically indistinguishable without nucleic acid
871 staining, populations of *C. sorokiniana* and toxic, PCC7806/ non-toxic, PCC9701 *M. aeruginosa*
872 were differentiated based on their intracellular fluorescence signals. (**B**) Flow cytometric
873 characterization of monoculture populations based on multiple cellular intrinsic properties, two of

874 which are presented in the panel (green fluorescence intensity vs. red fluorescence intensity). In
875 the flow cytometry (FCM) plots, points represent cells and warm to cool colors represent high to
876 low density based on the number of detected cells with those properties. Monoculture
877 populations have overlapping spectra patterns, and thus several cellular properties were
878 recorded for discrimination in bicultures. (**C**) At the top, select cellular properties derived from
879 FCM are compared against one another with the colors representing data from *C. sorokiniana*
880 (orange) and toxic *M. aeruginosa*, PCC7806 (purple) populations. Below, FCM data is used to
881 train a Random Forest classifier that is able to differentiate between populations with 99%
882 accuracy, results of the model predictions are shown in the table.
883
884 **Figure 3**| Strain variation in the cyanobacterium *M. aeruginosa* alters the competitive interaction
885 with the green alga *C. sorokiniana* under axenic conditions. Two sets of competition
886 experiments were conducted under the same laboratory conditions, but at two separate time-
887 points tracking both the resident phytoplankton population (open circles) and the invading
888 population (filled in circles). (**A**) In the first experiment, the toxic *M. aeruginosa* strain, PCC7806,
889 capable of producing the microcystin toxin, but not the non-toxic strain, PCC9701, was able to
890 invade and proliferate into a steady-state population of *C. sorokiniana*. In the reverse
891 interaction, *C. sorokiniana* was not able to establish in PCC7806, however *C. sorokiniana* was
892 able to invade PCC9701. (**B**) In the second experiment, the *mycB*- mutant ("MUT PCC7806") of
893 the toxic *M. aeruginosa* strain, which is deficient in microcystin production, was able to invade
894 and establish in a steady-state population of *C. sorokiniana*, however *C. sorokiniana* was not
895 able to establish in the MUT PCC7806 population. There is no statistical difference between the
896 competitive interactions between the WT and MUT PCC7806 *M. aeruginosa* strains and *C.*
897 *sorokiniana*. Circles on the graph represent the mean phytoplankton density estimated by flow
898 cytometry of three biological replicates and error bars represent the standard error of the mean,
899 with exception of the PCC7806 invading *Chlorella*, in the first experiment, were one outlier is not

included in the average, but is represented on the graph as individual measurements across time.

Figure 4| The presence of host-associated bacteria altered the competitive interaction between variants of the cyanobacterium *M. aeruginosa* and the green alga *C. sorokiniana*. During the competition experiments, *C. sorokiniana* was not able to establish in PCC7806 in either axenic/xenic state and *C. sorokiniana* was only able to invade and persist in non-toxic *M. aeruginosa* PCC 9701 in the axenic state (p-value: <0.0001), while in the xenic state *M. aeruginosa* PCC 9701 resisted the invasion of xenic *C. sorokiniana*. In the reverse interaction, when *C. sorokiniana* was dominant, the toxic *M. aeruginosa* strain PCC7806, but not the non-toxic strain, PCC9701, was able to invade and proliferate in both the axenic and xenic states. Circles on the graph represent the mean phytoplankton density of the steady-state phytoplankton population (open circled) and the invading population (filled in circles), estimated by flow cytometry of each biological replicate. Error bars indicate the standard error of the mean. In the case of PCC7806 invading *C. sorokiniana*, one outlier replicate in both the axenic and xenic state was not included in the mean phytoplankton density, but the phytoplankton population densities are plotted in the graph. For the remaining two replicates, PCC7806 reached a higher final population density when invading *C. sorokiniana* in the xenic state, in comparison to the axenic state ($p \leq 0.05$).

Figure 5| The absence of host-microbiomes resulted in two-fold increase in the concentration of total microcystin (µg) per cell when toxic *M. aeruginosa* was introduced into a steady-state population of *C. sorokiniana*. Samples for total microcystin content (combined intracellular and extracellular) were quantified 15 days after the introduction of the invader using the Abraxis Microcystins/ Nodularins (ADDA) ELISA Kit. The total microcystin concentration per cell (µg/cell) populations in the axenic/xenic state was calculated by dividing microcystin content by the

926 population density of toxic *M. aeruginosa* PCC7806 determined by flow cytometry. Bars on the
927 graph represent a biological replicate of the axenic or xenic competitive interaction, a single
928 outlier replicate, for each the axenic and xenic state, was not included in this analysis. The
929 single asterisk represents a p-value of 0.02 and indicates the phytoplankton cultures'
930 axenic/xenic state significantly affected microcystin concentrations, determined by performing
931 an analysis of variance on a linear mixed model on the data.
932
933 **Table 1**| Bacteria isolated from xenic populations of the corresponding phytoplankton species
934 were characterized by colony morphology and Sanger sequencing of the 16S rRNA gene.
935 Sequences were compared to the NCBI Genbank database using BLASTn and the bacterial
936 isolates with the highest percent identity are listed. Xenic phytoplankton populations used in our
937 study were engineered by adding isolates 1 and 2 to *C. sorokiniana* UTEX 2805 and isolates 3-
938 5 to toxic *M. aeruginosa* PCC 7806 and non-toxic *M. aeruginosa* PCC 9701.
939
940 **Table 1.**

Isolate #	Algal Host	Morphological Description	Family ID	Spp. ID (Perc. Ident.)
1	*C. sorokiniana*	Shiny, slimy, yellow	*Comamonadaceae*	*Variovorax paradoxus (96%)*
2	*C. sorokiniana*	Smooth, round, yellow	*Sphingobacteriaceae*	*Pedobacter glacialis (96.5%)*
3	LE3 *M. aeruginosa*	Semi-translucent, yellow, non-distinct edges	*Nocardioidaceae*	*Aeromicrobium ponti (97%)*
4	LE3 *M. aeruginosa*	White, cloudy	*Rhizobiaceae*	*Rhizobium* sp. (96.8%)
5	LE3 *M. aeruginosa*	Bright orange	*Sphingomonadaceae*	*Blastomonas fulva (97%)*

941

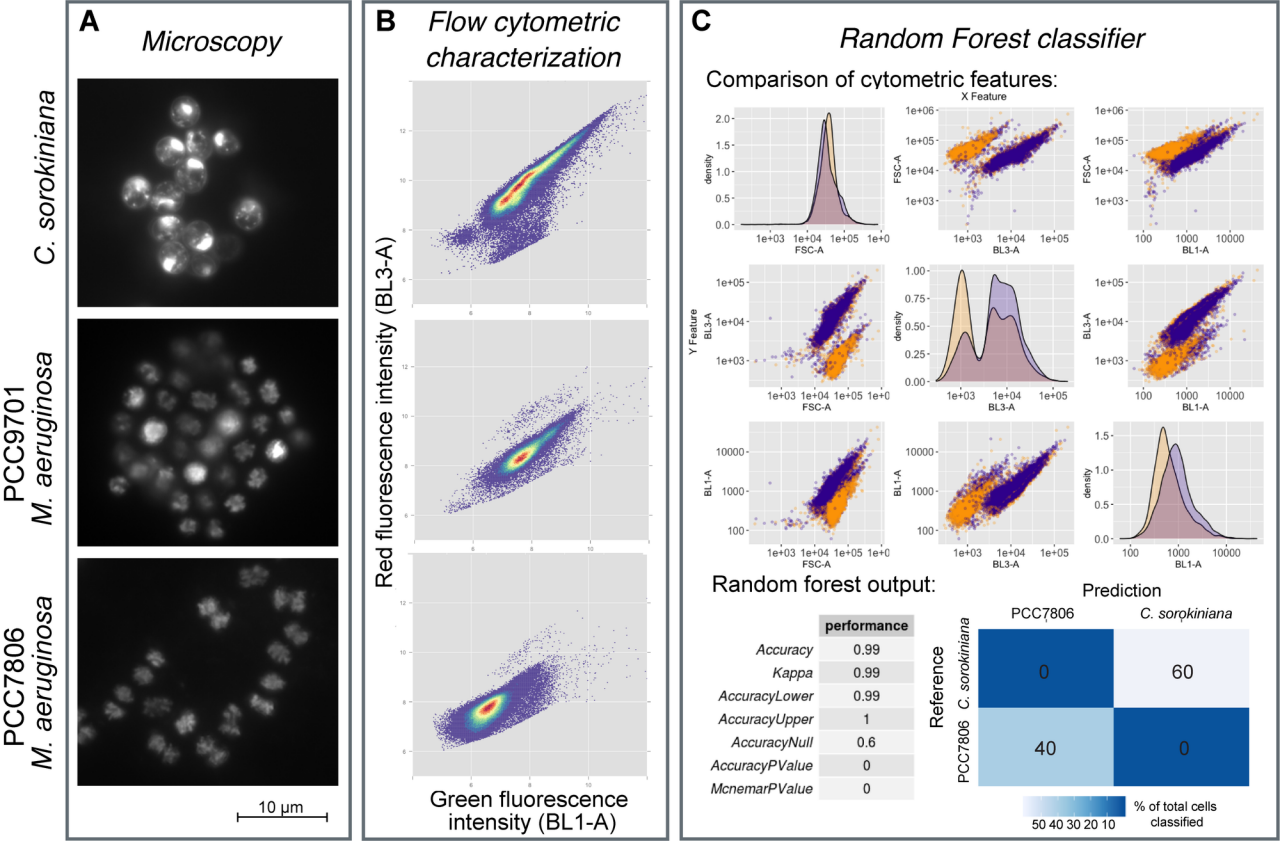
A
Microscopy
C. sorokiniana
PCC9701
M. aeruginosa
PCC7806
M. aeruginosa
10 µm
B
Flow cytometric characterization
Red fluorescence intensity (BL3-A)
Green fluorescence intensity (BL1-A)
C
Random Forest classifier
Comparison of cytometric features:
X Feature
Y Feature
density
FSC-A
BL3-A
BL1-A
Random forest output:
performance
Accuracy 0.99
Kappa 0.99
AccuracyLower 0.99
AccuracyUpper 1
AccuracyNull 0.6
AccuracyPValue 0
McnemarPValue 0
Prediction
PCC7806
C. sorokiniana
Reference
0
60
40
0
% of total cells classified
50 40 30 20 10

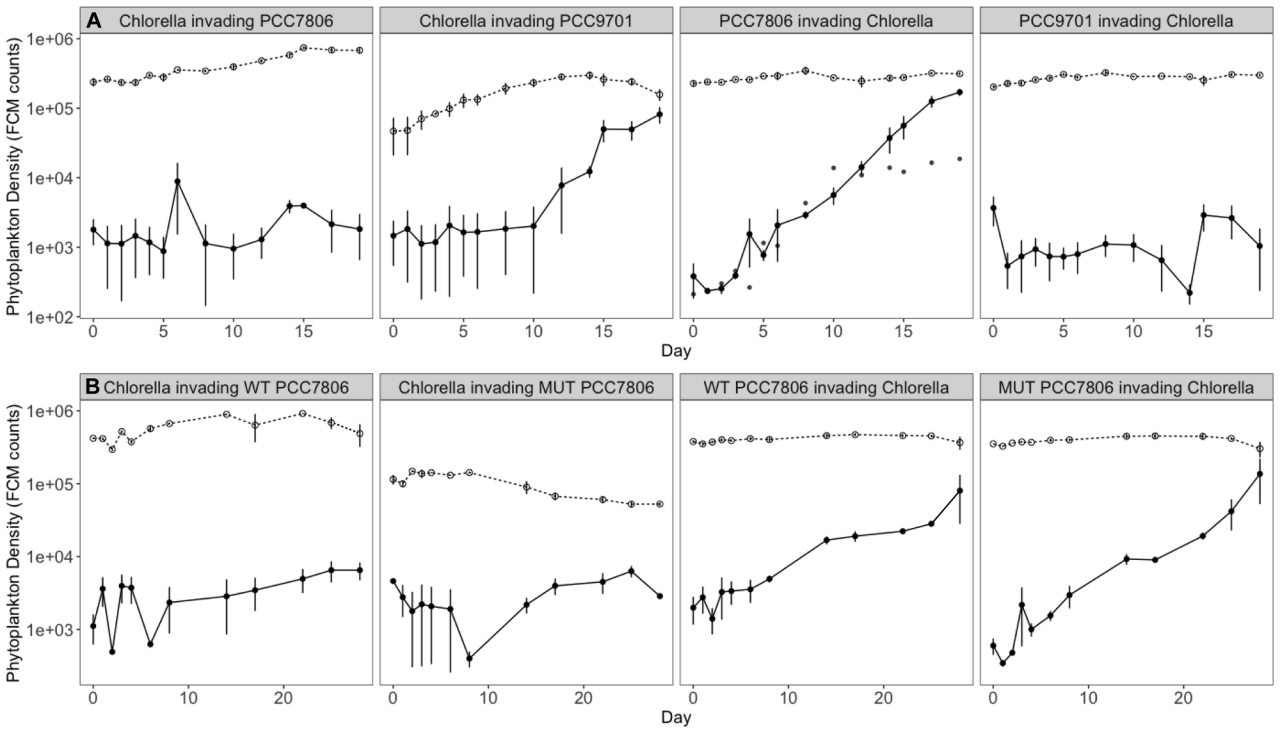
A
Chlorella invading PCC7806
Chlorella invading PCC9701
PCC7806 invading Chlorella
PCC9701 invading Chlorella
B
Chlorella invading WT PCC7806
Chlorella invading MUT PCC7806
WT PCC7806 invading Chlorella
MUT PCC7806 invading Chlorella
Phytoplankton Density (FCM counts)
1e+02
1e+03
1e+04
1e+05
1e+06
0
5
10
15
20
Day

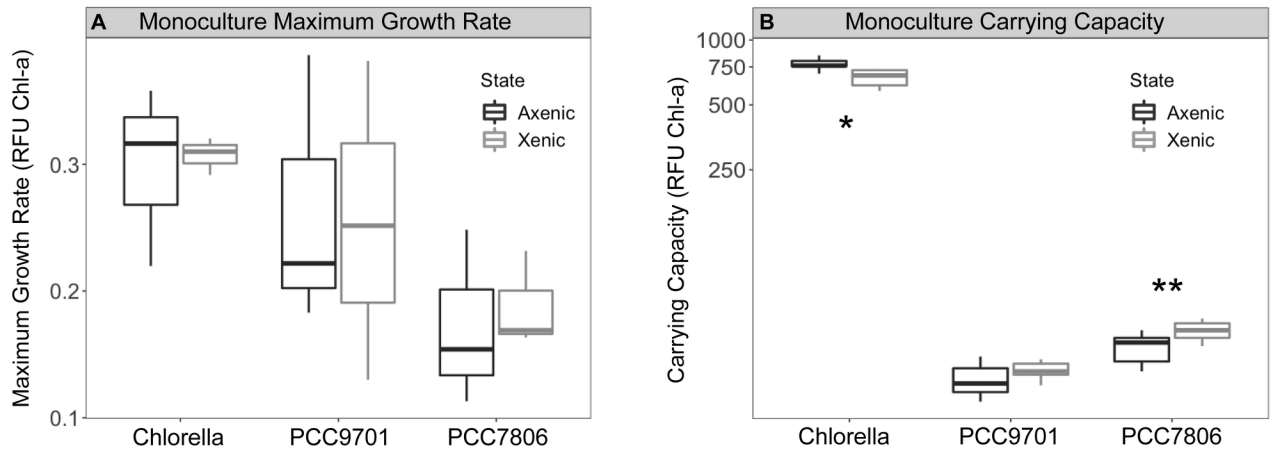
A
Monoculture Maximum Growth Rate
Maximum Growth Rate (RFU Chl-a)
0.3
0.2
0.1
State
Axenic
Xenic
Chlorella
PCC9701
PCC7806
B
Monoculture Carrying Capacity
Carrying Capacity (RFU Chl-a)
1000
750
500
250
State
Axenic
Xenic
*
**
Chlorella
PCC9701
PCC7806

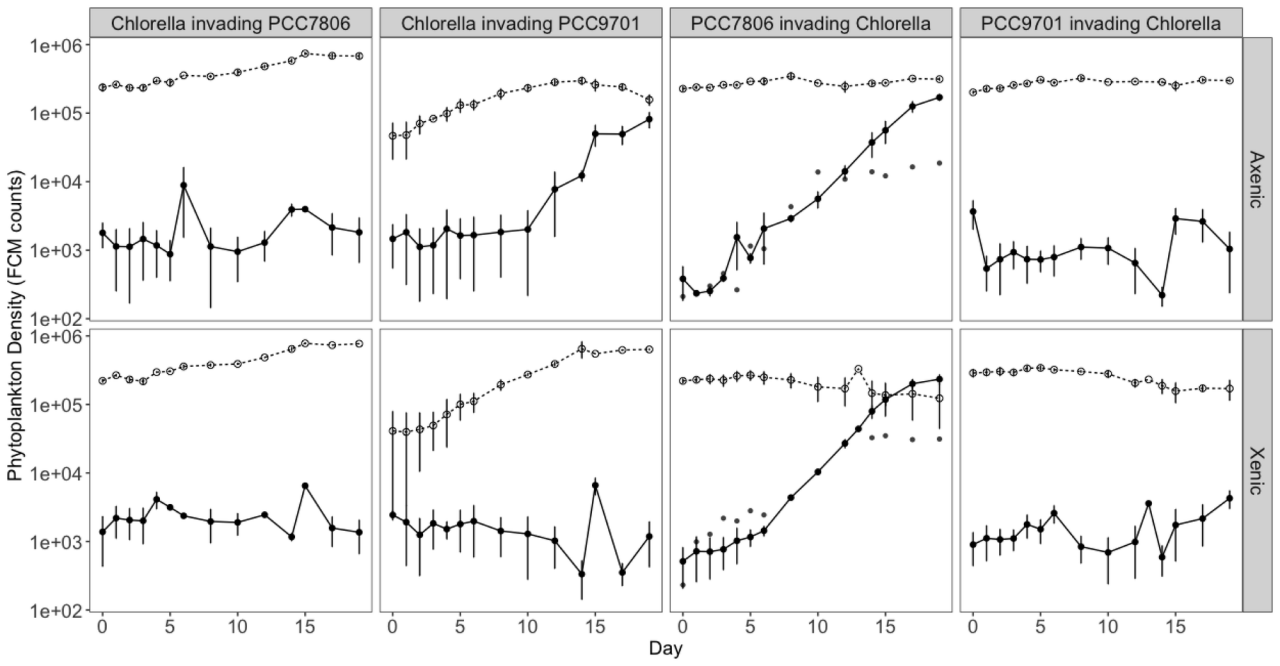
Chlorella invading PCC7806
Chlorella invading PCC9701
PCC7806 invading Chlorella
PCC9701 invading Chlorella
Axenic
Xenic
Phytoplankton Density (FCM counts)
1e+06
1e+05
1e+04
1e+03
1e+02
0
5
10
15
Day

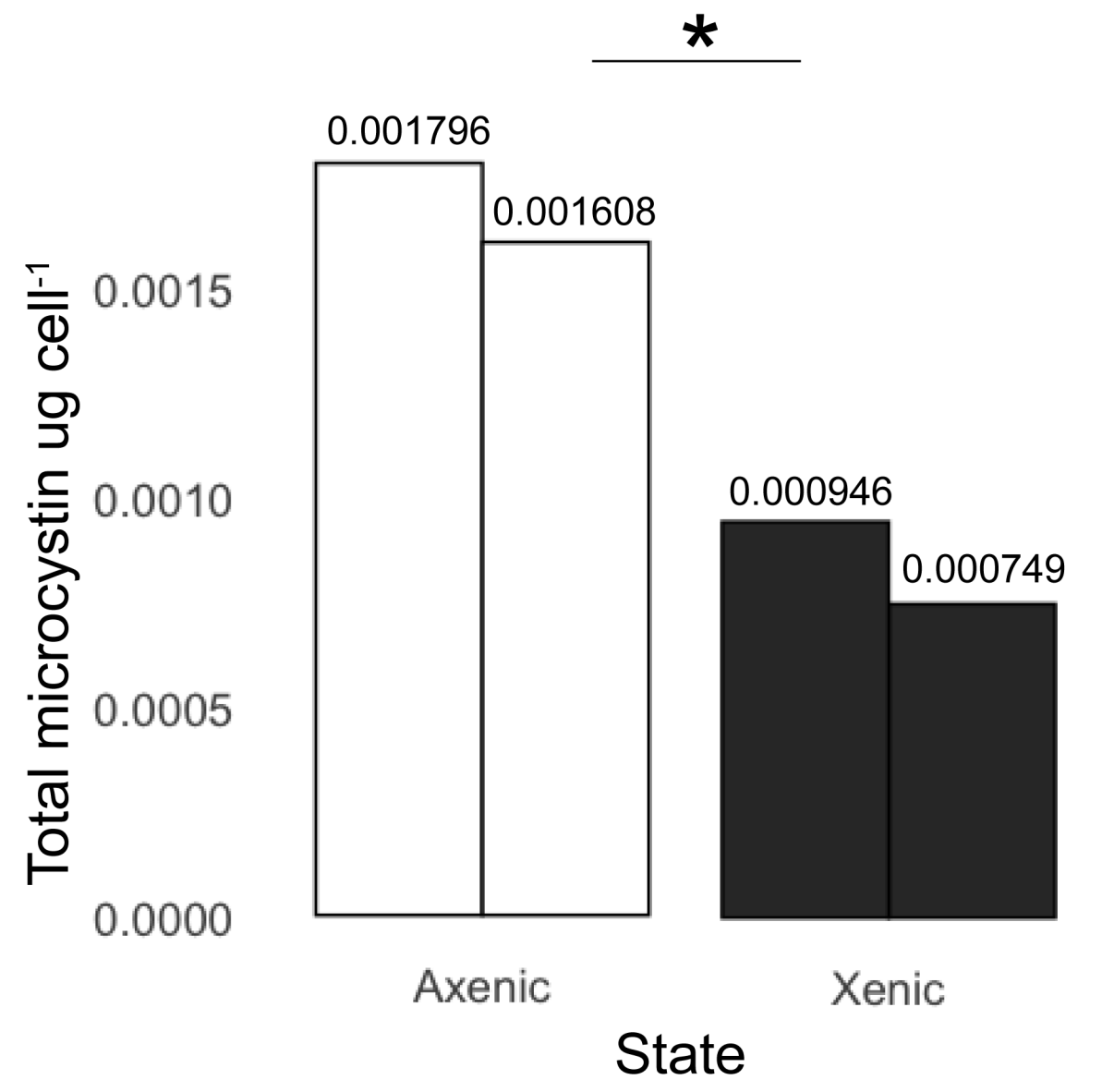
*
0.001796
0.001608
0.000946
0.000749
0.0015
0.0010
0.0005
0.0000
Total microcystin ug cell-1
Axenic
Xenic
State